

INJECTION and RF CAPTURE in the NSNS
A NUMERICAL SIMULATION IN 6 DIMENSIONS

BNL/NSNS TECHNICAL NOTE

NO. 004

A. U. Luccio, D. Maletic and F. W. Jones

December 5, 1996

ALTERNATING GRADIENT SYNCHROTRON DEPARTMENT
BROOKHAVEN NATIONAL LABORATORY
UPTON, NEW YORK 11973

INJECTION AND RF CAPTURE IN THE NSNS A NUMERICAL SIMULATION IN 6 DIMENSIONS *

A.U.LUCCIO, D.MALETIC

AGS Department, Brookhaven National Laboratory, Upton, NY 11973, USA

F.W. JONES

TRIUMF, 4004 Wesbrook Mall, Vancouver, B.C., Canada V6T 2A3

1. Introduction

In its present design, the National Spallation Neutron Source consists of a 1 GeV proton linac followed by an accumulator ring¹. To produce neutrons, the protons are made to strike a target. The challenge of the accumulator design reflects the need for high currents (1 mA).

A computer simulation study of the injection and RF capture processes in a 1 MW accumulator ring was performed with the code *Accsim*, developed at TRIUMF². The simulation is fully 6-dimensional, with tracking of a certain number of macro particles through the lattice, in the presence of space charge forces and beam to wall interaction. One starts with an initial random distribution of the macro particles in the transverse and longitudinal phase spaces. Then, the tracking is continued by representing the lattice with a number of transfer matrices obtained with the codes *Mad*³ and *Dimad*⁴.

Main goals of the simulation were: (i) limit particle losses in order to avoid radiation contamination, (ii) inject a long pulse to decrease the average current to be delivered by the linac, (iii) try different RF types and injection strategies, and (iv) experiment with various beam energy spreads, and with beams carrying some halo.

The linac accelerates H^- ions. The H^- are stripped to H^+ and injected in the ring. *Accsim* calculates the scattering in the injection foil, that is traversed a few times by the injected and stored beam during the first turns.

Losses arise from two main sources: H^- ions missing the foil, or not being converted to protons, and protons hitting the walls during the accumulation process. *Accsim* counts lost particles and takes them off the tracking cycle. A general strategy was to try to limit the losses to a region close to the foil, where it is easy to insert an appropriate dump (controlled losses) while trying to avoid spilling in other regions of the ring. Since we plan to extract the beam immediately after the injection is completed, the beam will not have time to diffuse and consequently losses will be reduced.

The number of macroparticles used in the simulation generally varies between 10^4 and 10^6 . A limit on this number is set by the computer time needed to complete a tracking run. On our Silicon Graphics Challenge M Server, a typical running time was

*Work performed under the auspices of the US Department of the Energy

from 20 minutes to a few hours, respectively. Here, we used 12,000 macroparticles.

2. Machine lattice. Matrices. Mad. Dimad.

The lattice of the SNS Accumulator ring is described elsewhere ⁵. The super symmetry of the lattice is 3. It consists of an array of FODO cells, 208.558 m long, with three straight sections, for injection, extraction and to accommodate the RF cavity, respectively.

In the *Accsim* simulation, to account for possible beam losses against the accelerator chamber walls, a set of collimating apertures were placed at various points around the ring circumference, where the beam envelope is largest. For the present calculations, these apertures are $100 \times 100 \text{ mm}^2$ or $160 \times 160 \text{ mm}^2$ (in a few sections). More realistic values will be used in a further stage of the design.

The lattice was optimized with *Mad*. Then, *Dimad* was used to calculate the transfer matrices between a sequence of points around the ring and to produce an input file to *Accsim*. In total, 38 matrices were used in the simulation

3. Injection

The 1 GeV H^- beam from the linac is injected into the accumulator ring and converted to H^+ in a carbon stripping foil ($Z = 6, A = 12.01$). The foil dimensions are 6 mm (radial) \times 20 mm (vertical) and its thickness is $400 \mu\text{g}/\text{cm}^2$. The foil is centered on the location $x = 94 \text{ mm}, y = 16.7 \text{ mm}$ with respect to the vacuum chamber reference center. Dimensions, thickness and position of the foil are a result of some compromise between stripping and capture efficiencies and also by the need to limit and localize beam losses at injection ⁶.

In the foil, a plural tabulated scattering distribution ¹⁰ was used to generate scattering angles. Nuclear scattering is not currently directly simulated in *Accsim*.

At injection, the ring equilibrium orbit is distorted with a radial 5-magnet bump, as shown in Fig. 1. Initially, in correspondence to the foil, the radial bumped orbit is centered on the beam injection spot. The bump is made to partially collapse in time, so that at the end of injection the radial phase space acceptance center will be located at a smaller radius. The coordinates of the closed orbit vs. time are shown in Fig. 2. The final equilibrium orbit remains bumped at the end of injection and the final acceptance will just graze the foil edge. This situation is shown in Fig. 3. In the bump, 4 out of 5 magnets are ramped in time to accomplish the collapsing bump. The fifth, labeled B3 in Fig. 1 and located immediately after the foil, is kept at a constant value of the field. The reason for this is that, since some magnetic stripping may happen in the magnet B3 and we want to keep the ensuing losses at a minimum, the magnetic field should be maintained at an optimum value.

A possible vertical phase space at injection is shown in Fig. 4. In order to control the filling of the vertical acceptance, we have also investigated the possibility of vertical painting, since it is unpractical to produce a vertical orbit bump for lack of space. To achieve painting in the vertical phase space, the beam should be steered in the injection line, while the circulating beam is kept vertically fixed. The resulting vertical phase space pattern is shown in Fig. 5. Parameters for the radial orbit bump and vertical painting are given in Table I

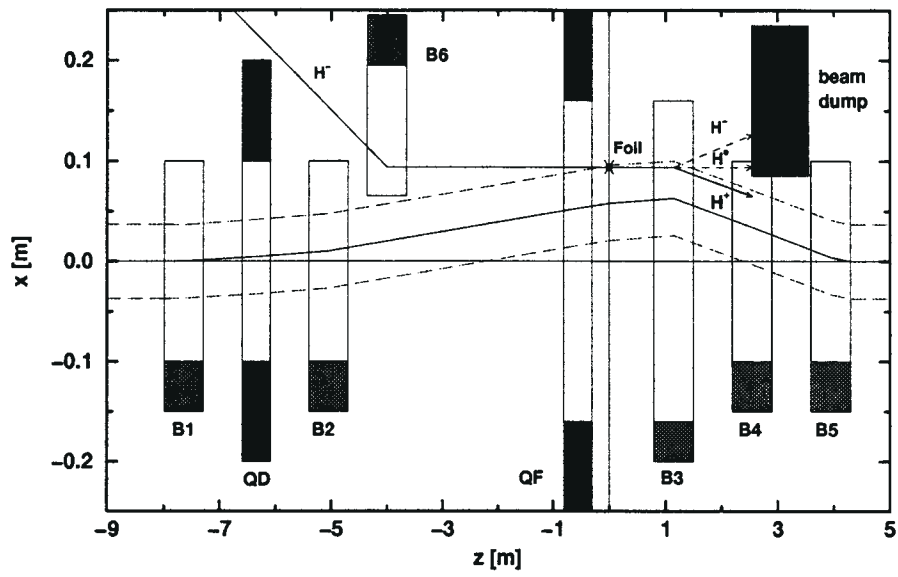


Figure 1: Layout of the injection 5-magnet radial bump.

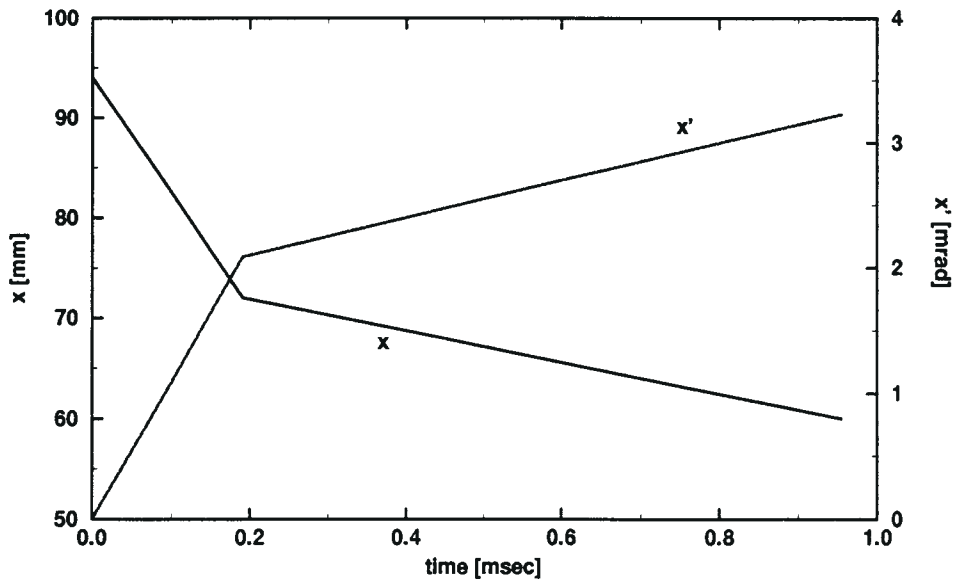


Figure 2: Coordinates of the injection radial bump, at the foil.

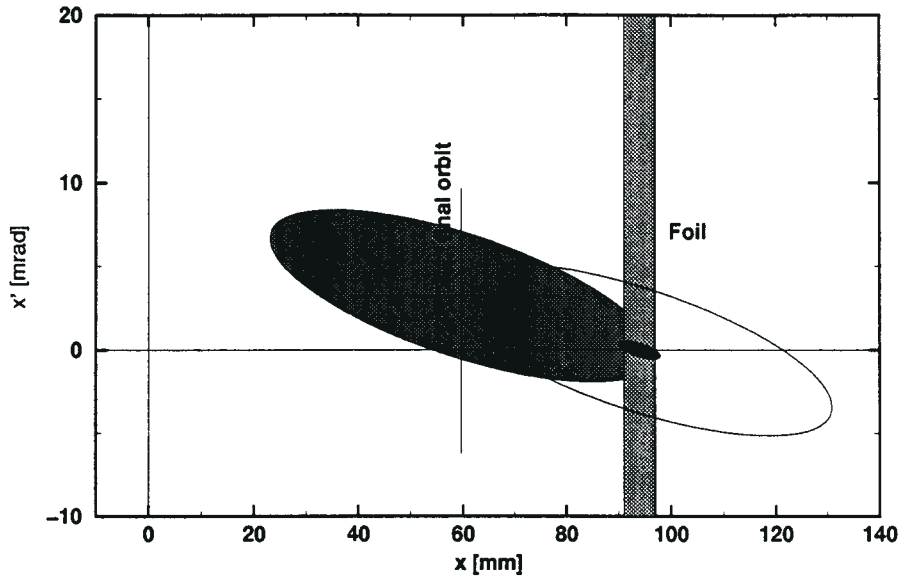


Figure 3: Radial phase space during injection. Injected beam (solid small ellipse), initial acceptance (right ellipse) and final acceptance (left ellipse) are shown.

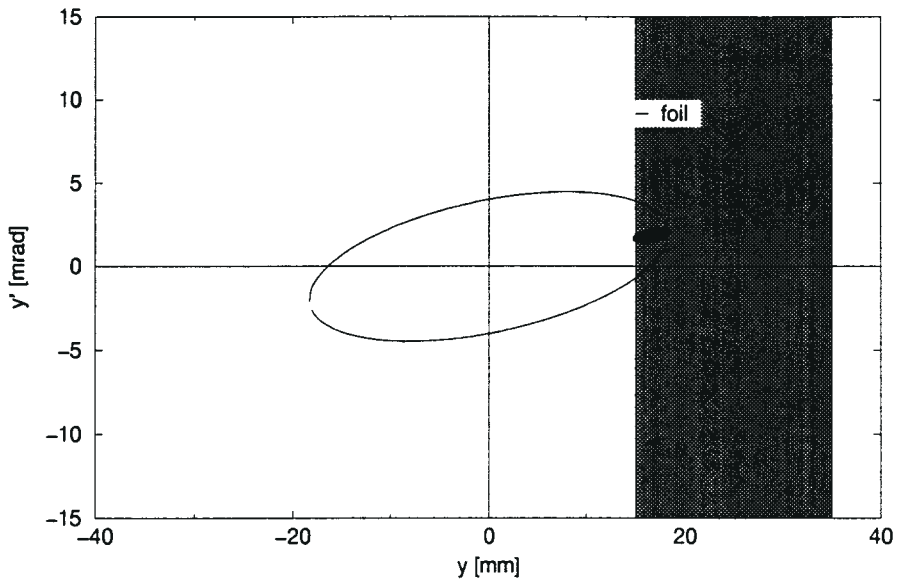


Figure 4: Vertical phase space during injection. No vertical painting.

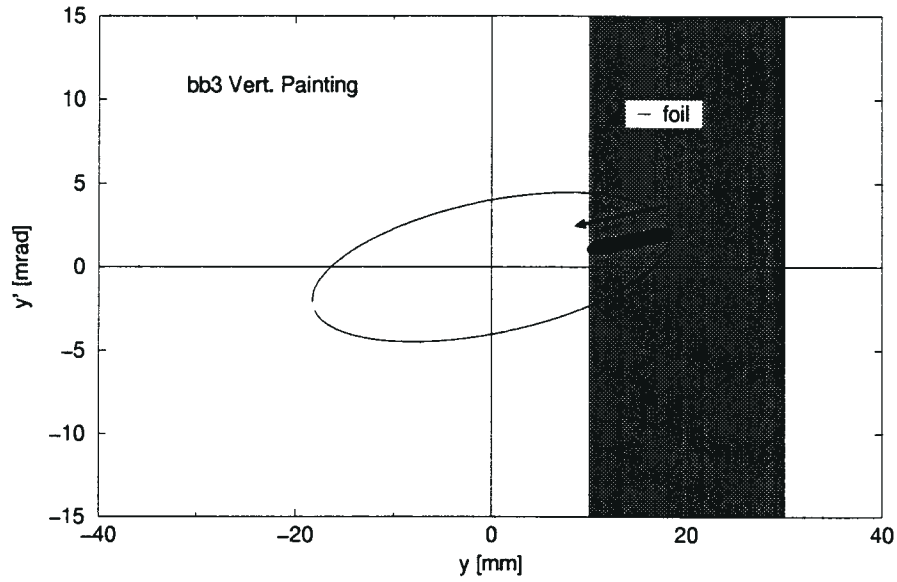


Figure 5: Vertical phase space during injection. Vertical painting.

Table I: Radial and vertical injection. Orbit bump and painting.

Radial orbit bump:			
time [msec]	0	0.191	0.954
x_c [mm]	94	72	60
x'_c [mrad]	0	2.09	3.229
Radial injection at:			
x_0 [mm]	94		
x'_0 [mrad]	0		
Vertical orbit:			
y_c [mm]	0		
y'_c [mrad]	0		
Vertical injection (no painting) at:			
y_0 [mm]	0		
y'_0 [mrad]	0		
Vertical injection (painting) at:			
time [msec]	0	0.191	0.954
y_0 [mm]	16.7	14.20	11.70
y'_0 [mrad]	1.88	1.58	1.28

Table II: Parameters of the injected beam in the accumulator.

	α	β [m]	ϵ [mm-mrad]
radial phase space:	2.0995	22.149	0.35
vertical phase space:	-0.5909	5.411	0.35
longitudinal phase space:	$\Delta\phi = 240$ or 200 [deg] $dE/E=0.0016$		

During injection, the injection line dispersion was matched to the ring dispersion at the foil. Among the other twiss functions, only α , i.e. the phase space tilt, was matched, while we tried several β values, both radial and vertical. Injected beam parameters are given in Table II.

The distribution of macro particles at injection is taken as random gaussian in the radial and vertical phase space and flat in the longitudinal phase. The values for the transverse emittance shown is for 2σ .

The injected number of protons in the accumulator ring is 1.042×10^{14} , corresponding to a beam power of 1 MW. The injection takes about 1 msec, or 1,200 turns. This number of turns and the longitudinal phase bite injected, 240° or $2/3$ of the bucket, were chosen to best match the linac beam structure. In some cases, we tried a shorter bunch, i.e. $\Delta\phi = 200^\circ$. At the present time, no effort was made to include in the calculation the microbunch structure of the linac beam.

4. RF Capture. Tune shift, losses

At the present stage of evolution of the accumulator design, we plan to extract the beam immediately at the end of the 1,200 turn injection process. So, we are not interested in long term beam accumulation and RF capture beyond 1 msec.

For such a high intensity beam, its size and stability during injection and RF capture are strongly affected by space charge. Tune shifts and tune spread are indicative of transverse space charge effects and should be kept as small as possible. A design limit for transverse tune shift, both radial and vertical, is $\Delta\nu = -0.2$. Following our experience with AGS operation, and in agreement with previous calculations¹², we decided to operate with a rather hollow, or "smoke ring" beam. The injection scheme previously described was designed to accomplish that, both in the radial and vertical phase spaces, filling the acceptance by controlling the position of the injected beam in a moving acceptance phase space ellipse, as done in the radial phase space, or by moving the beam (painting) in the acceptance, as done in the vertical phase space.

The transverse tune shift is calculated in *Accsim* with a formalism which computes the amplitude dependent tune shift due to the space charge forces of the instantaneous 2-dimensional betatron amplitude distribution⁸.

A treatment of the space charge induced transverse tune shift with straightforward electro magnetic considerations, based on an earlier (Bruck-Laslett) formulation⁹, brings to the following expression of the maximum tune shift in either transverse direction

$$\delta\nu = -\frac{r_0 N}{\beta^2 \gamma^3} \frac{R}{2\pi\nu} P \quad (1)$$

where N is the number of particles in the beam per unit transverse area, R is the

average machine radius, β and γ the relativistic factors, and P a beam form factor that takes into account also the longitudinal beam bunching. r_0 is the classical proton radius and ν the betatron tune.

Eq. (1) is well reproduced by *Accsim* when the beam transverse profile has only one peak, like in a gaussian distribution, and when the effects of the other dimension(s) can be neglected. However, in the more general case, e.g. when a distribution with more peaks is present, like in a smoke ring, the agreement with Eq. (1) is dubious. In this case, the maximum tune shift loses some of its meaning, while a tune shift spread is more appropriate. We need to bear in mind these considerations in the analysis of simulation data.

In the longitudinal phase space, to accomplish the capture of the injected beam at constant energy into a stable bucket, the accumulator is being furnished with a RF system. Three RF types have been considered and simulated: 1.st Harmonic, 1.st + 2.nd harmonic and Barrier RF. They will be described in the next Section.

The effect of space charge in the longitudinal dynamics is included in *Accsim*. The space charge induced additional voltage on the beam (other than the RF's) is calculated by binning and smoothing the longitudinal beam profile and assuming an impedance corresponding to a perfectly conducting smooth chamber wall. In this assumption, the on-axis longitudinal space charge field can be calculated with the expression ¹¹

$$V_{sc} = -\frac{Z_0 c}{4\pi} \left(1 + 2 \ln \frac{b}{a}\right) \frac{d\lambda}{ds} \quad (2)$$

with Z_0 the impedance of free space, $d\lambda/ds$ the longitudinal gradient of the electric charge in the beam, and b/a the ratio between beam and chamber (assumed round) radii. In our simulation, we took $b/a = 3$.

At the present stage of design, no detailed impedance budget was considered, but we plan to account for it at a later time. However, since the tune shifts appears to be mostly dominated by transverse space charge, we don't anticipate a large effect.

4.1. 1.st Harmonic RF Cavity

A cavity and RF system operating on the 1.st (or fundamental) harmonic at a frequency of 1.258 MHz are straightforward. In this case, we found good results with a peak accelerating voltage of 30 KV. The resulting bucket area was ~ 10 eV-sec. We didn't observe any beam losses in excess of 10^{-4} during the 1,200 turns of injection and capture, and the beam seemed to still maintain a good integrity at that time. Transverse emittance tune shifts were well contained within the design limits of -0.2. Actually, with no vertical painting, in this simulation the vertical tune shift was very small due to the very narrow smoke ring configuration achieved. Results will be shown in the following sections.

4.2. 1.st + 2.nd Harmonic RF Cavity

Adding a 2.nd harmonic to the RF system improves the longitudinal phase space and the transverse tune shift ⁷. We tried this case that creates a more compact beam. Cavity voltage is shown in Fig. 6. We added to the 1.st harmonic voltage of 40.34 KV

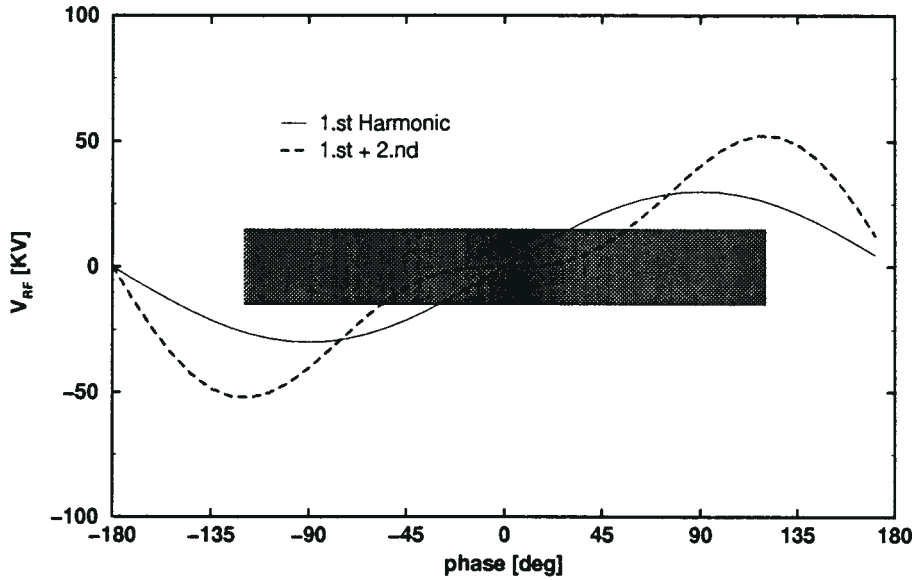


Figure 6: 1.st Harmonic (solid line), and 1.st + 2.nd Harmonic Cavity Voltage (dashed line). A 240° beam bunch is also diagrammatically shown

a 2.nd harmonic of amplitude 20.17 KV.

4.3. Barrier RF Cavity

The other RF option being considered is a barrier cavity RF system ⁷. The simulation showed that this option allows one to obtain a smaller radial tune shift, as the theory predicts. In this case, we also allowed vertical painting, that shows its effect on the vertical tune shift (with the caveat on the meaning of transverse tune shift numbers expressed earlier in this section).

Barrier cavity voltage is shown in Fig. 7. The voltage is strictly zero between the two 80 KV voltage peaks. Peak amplitude is 90° , corresponding to a RF harmonic of 2 (a higher harmonic would be more difficult to obtain in pulse power). Note also that a similar voltage could be constructed adding to a fundamental RF frequency a second and third harmonics with amplitudes of 43.36117, 40.01640, and 12.45771 KV, respectively, yielding a total peak voltage of ~ 80 KV.

5. Results of the *Accsim* simulation

5.1. 1.st Harmonic RF. No vertical painting

Snapshots of the beam at 600 and 1,200 turns are shown in Figs. 8 and 9. The five diagrams represent, from left to right and from top to bottom the beam distribution in

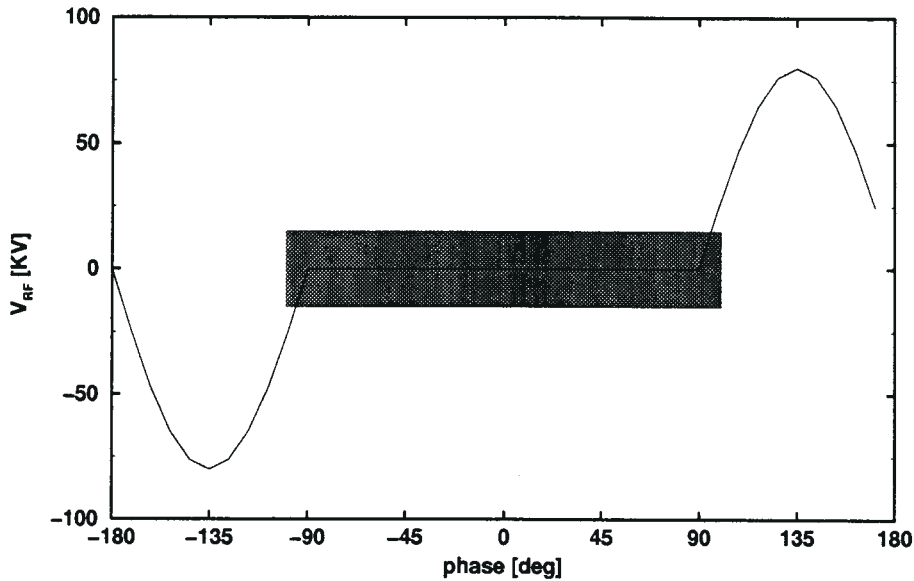


Figure 7: Barrier Cavity Voltage. A 200° bunch is also shown.

the radial and vertical phase space, the longitudinal voltage due to the space charge, the cross section of the beam in real space (this diagram also shows the location of the stripping injection foil) and the beam distribution in longitudinal phase space. The bucket separatrix is also represented in the latter diagram.

In this case, few particles miss the foil at injection and produce a controlled beam loss that will be dumped. No further losses were found against the chamber walls.

Fig. 10 shows the resulting radial and vertical emittance and tune shifts.

5.2. 1.st + 2.nd harmonics. No vertical painting

Snapshots of the beam at 600 and 1,200 turns are shown in Figs. 11 and 12. The tight bucket and halo formation, due to the wide (240°) phase extension of the beam bunch, are evident from the figures.

Fig. 13 shows the resulting radial and vertical emittance and tune shifts.

5.3. Barrier RF. No vertical painting

The barrier waveform is creating a much more compact bunch. In order to decrease the halo, the length in phase of the injected bunch has been reduced in this examples to 200° , as diagrammatically shown in Fig. 7. Work is in progress to optimize the RF voltage waveform in order to further decrease the halo. The option of shortening the beam phase length is not too attractive, because it will decrease the efficiency of the beam delivered by the linac.

Snapshots of the beam at 600 and 1,200 turns are shown in Figs. 14 and 15 using

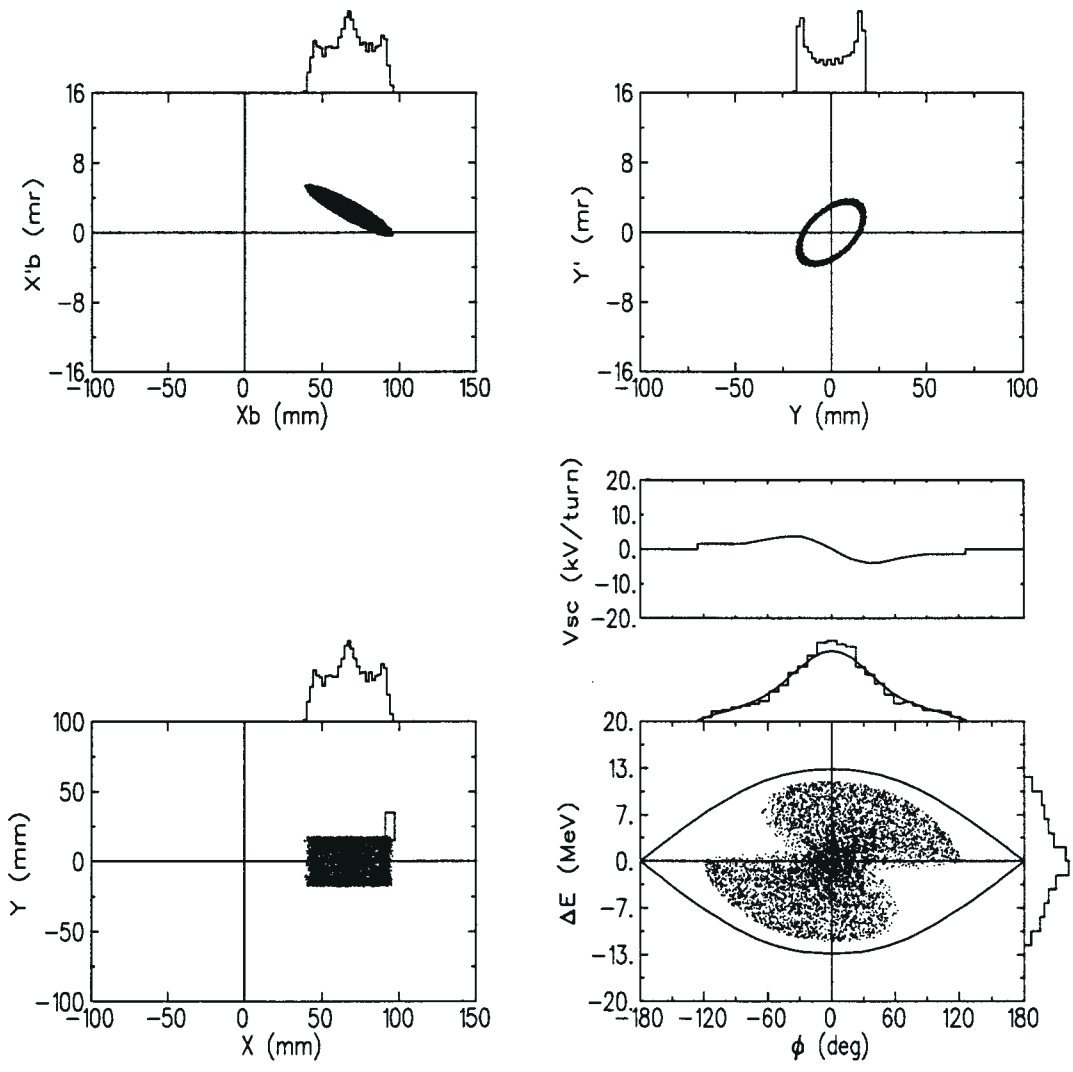


Figure 8: Snapshots at 600 turns. 1st harmonic RF. No vertical painting.

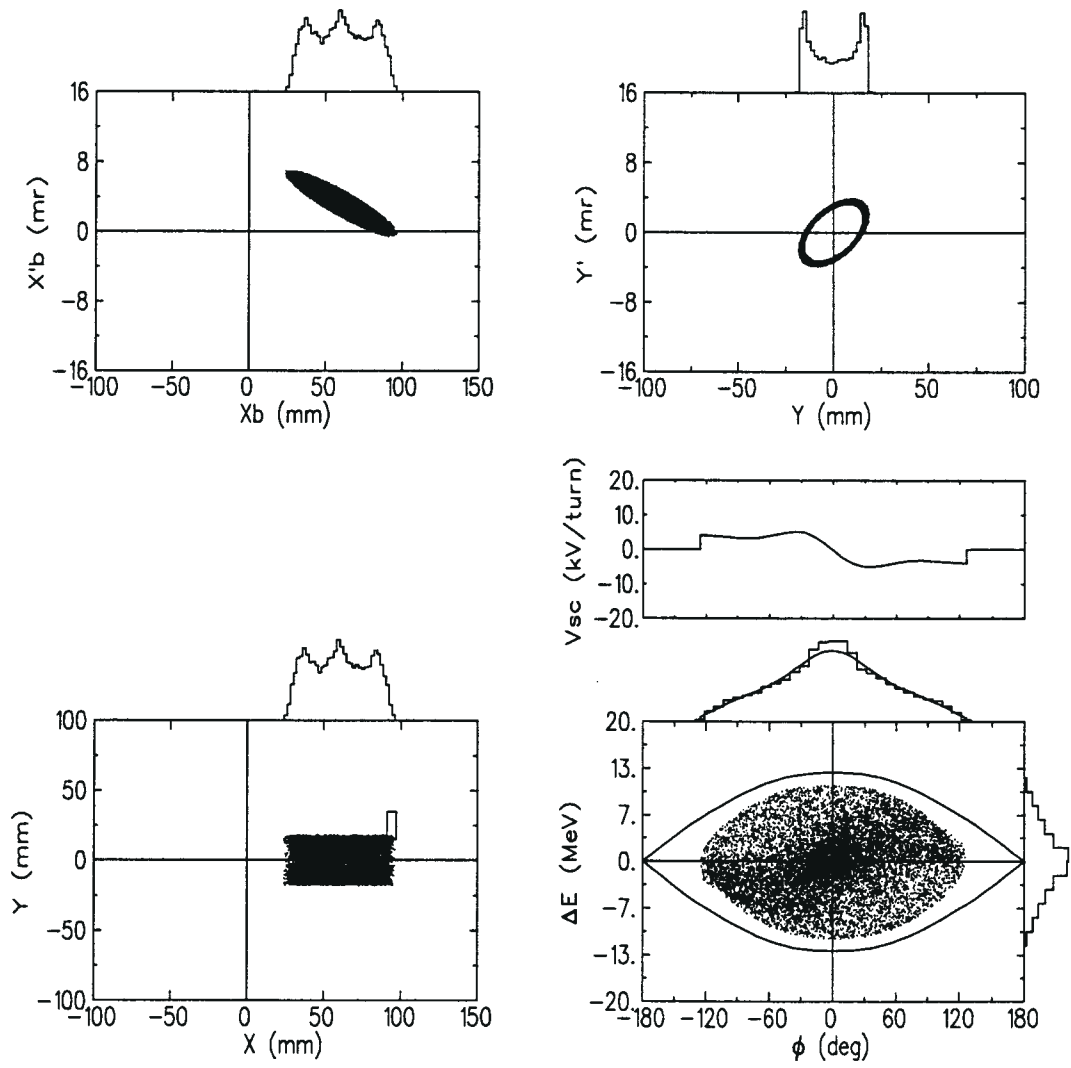


Figure 9: Snapshots at 1,200 turns. 1.st harmonic RF. No vertical painting.

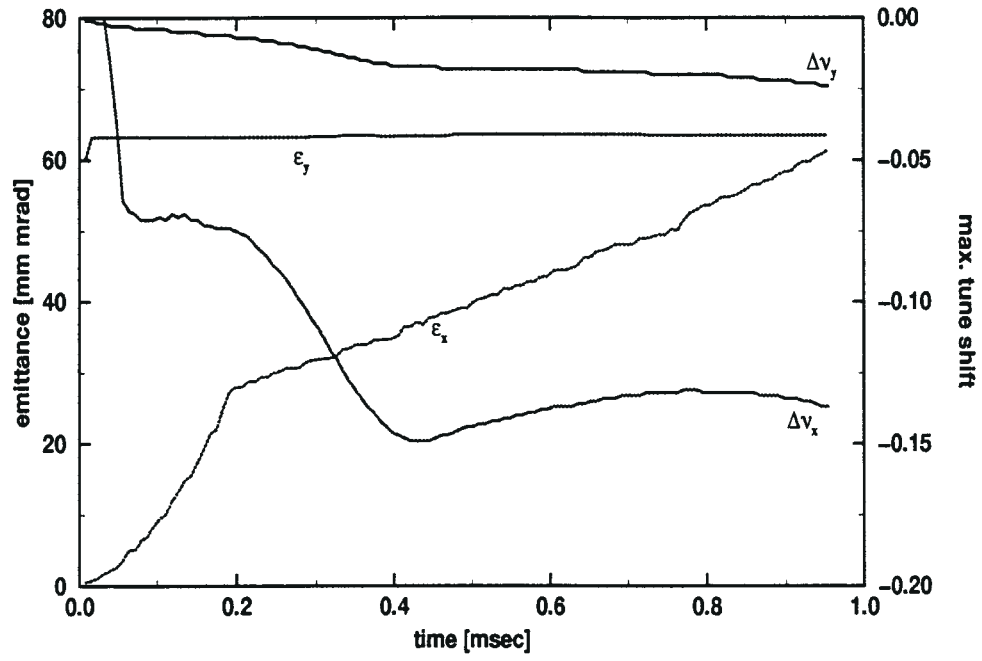


Figure 10: Transverse emittance and tune shift. 1.st harmonic RF.

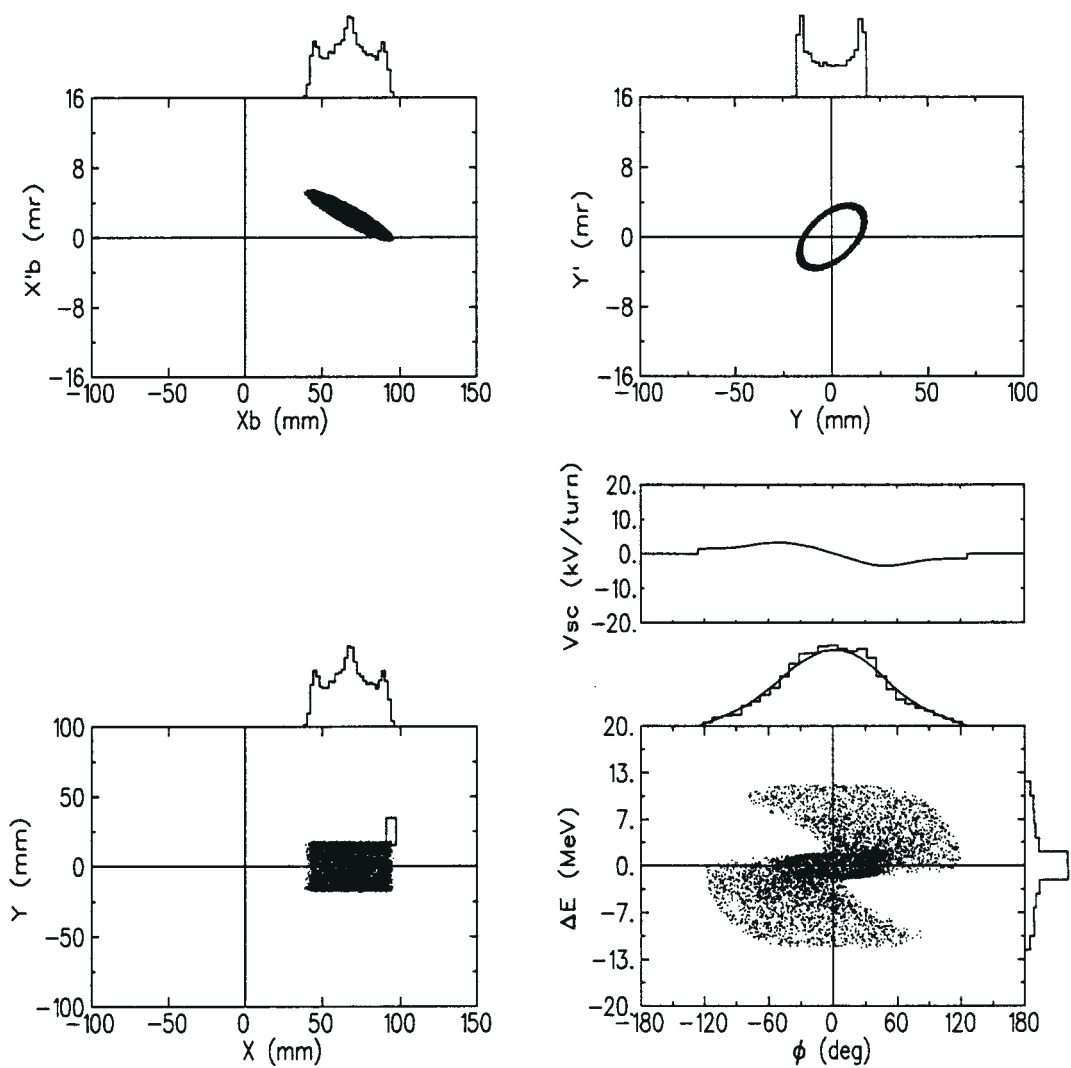


Figure 11: Snapshots at 600 turns. 1.st + 2.nd harmonics RF. No vertical painting.

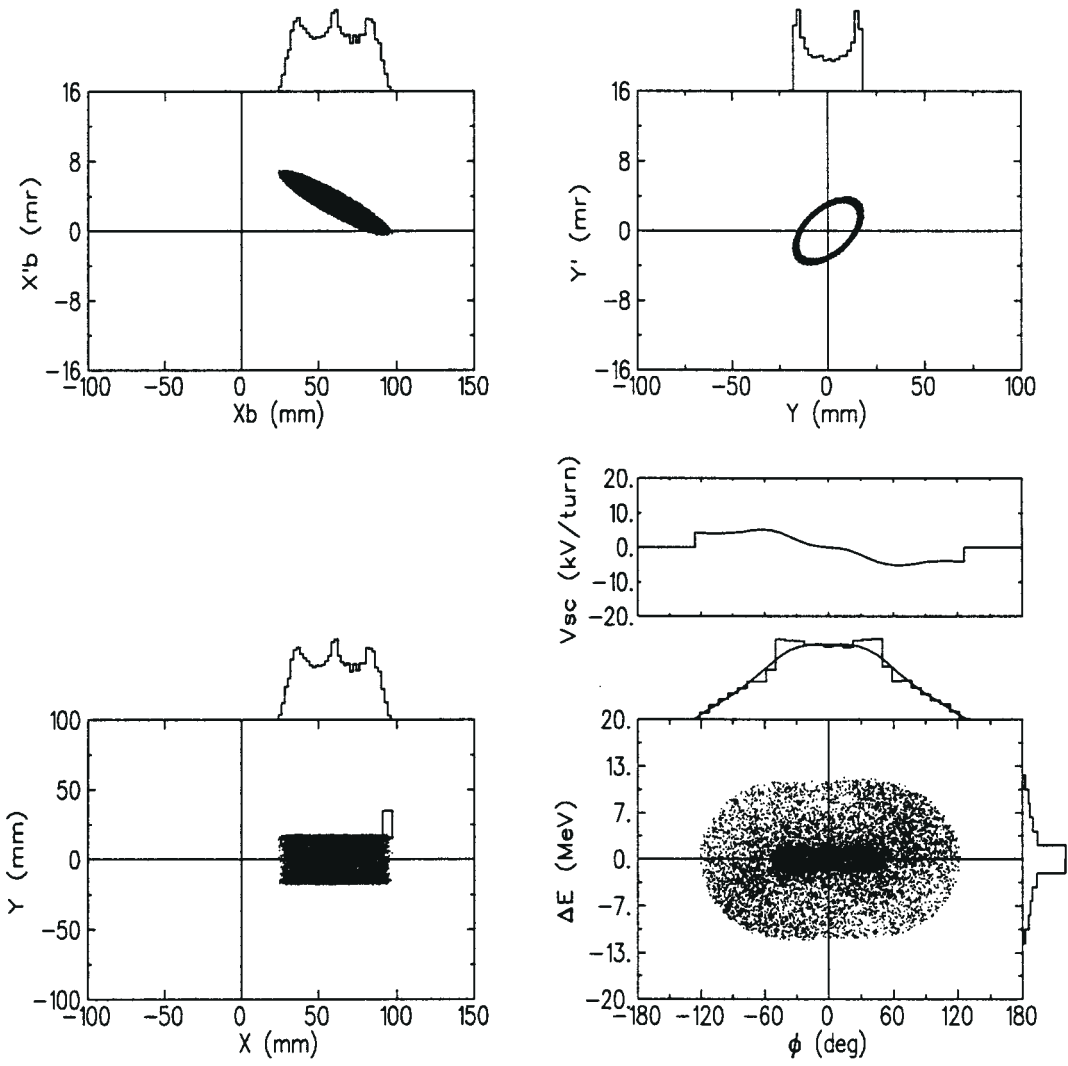


Figure 12: Snapshots at 1,200 turns. 1.st + 2.nd harmonics RF. No vertical painting.

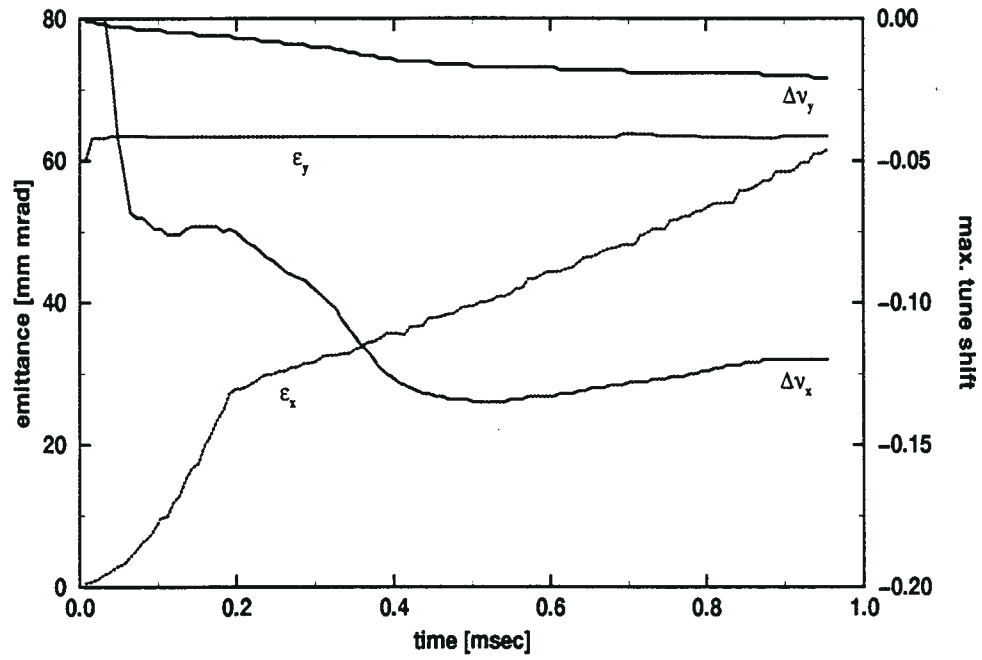


Figure 13: Transverse emittance and tune shift. 1.st + 2.nd harmonics RF.

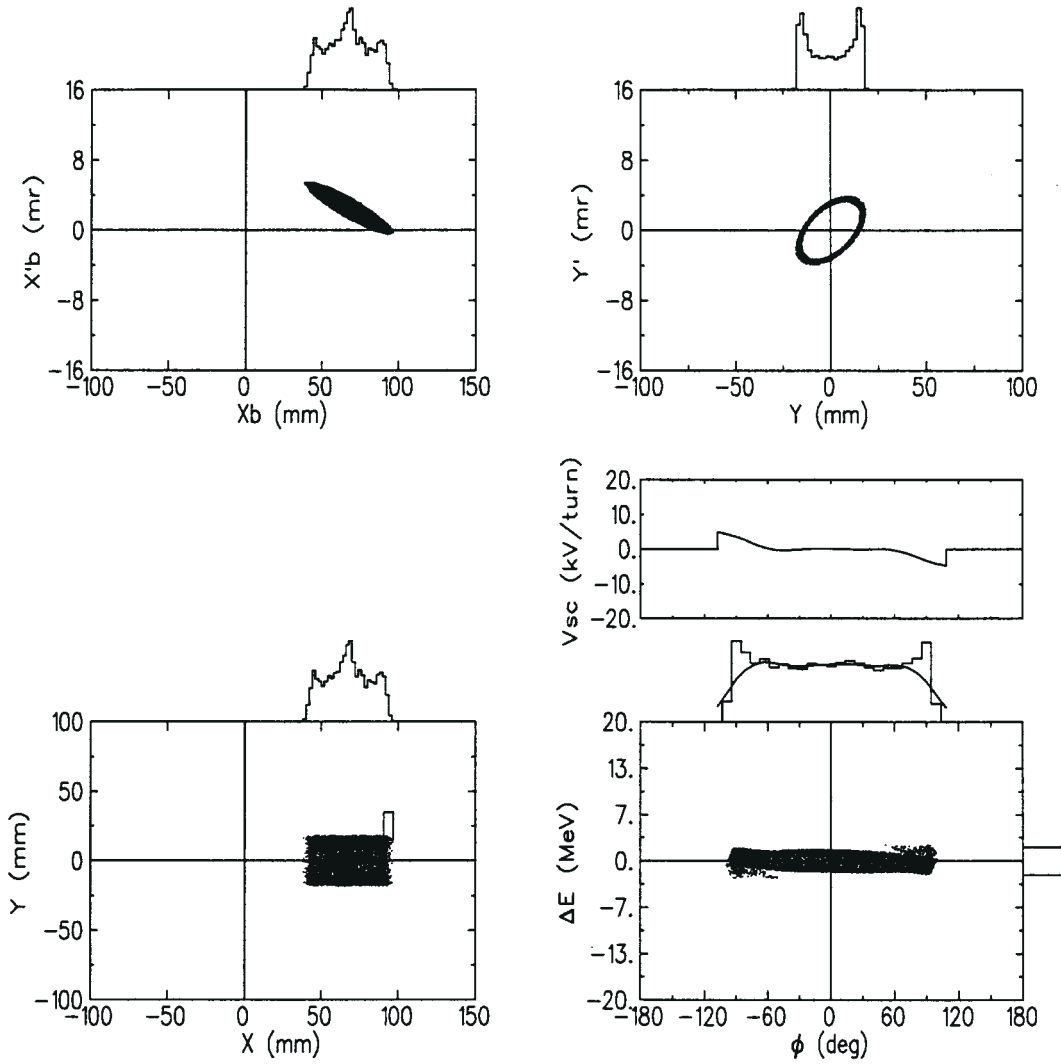


Figure 14: Snapshots at 600 turns. Barrier RF. No vertical painting.

a barrier cavity with the voltage waveform shown in Fig. 7. The tight bucket and almost no halo formation are evident from the figures.

Fig. 16 shows the radial and vertical emittance and tune shift. A comparison with Fig. 10 shows a substantial reduction of the radial tune shift due to the effect of the RF barrier.

5.4. Barrier RF. With vertical painting

Snapshots of the beam at 600 and 1,200 turns are shown in Figs. 17 and 18 using a barrier cavity with the same voltage waveform as before. In this case we considered vertical painting, in order to create a “thicker” smoke ring in vertical space and avoid possible instabilities that may arise when the local charge density is very high. Fig. 5 shows the vertical acceptance and injected beam during vertical painting for this case.

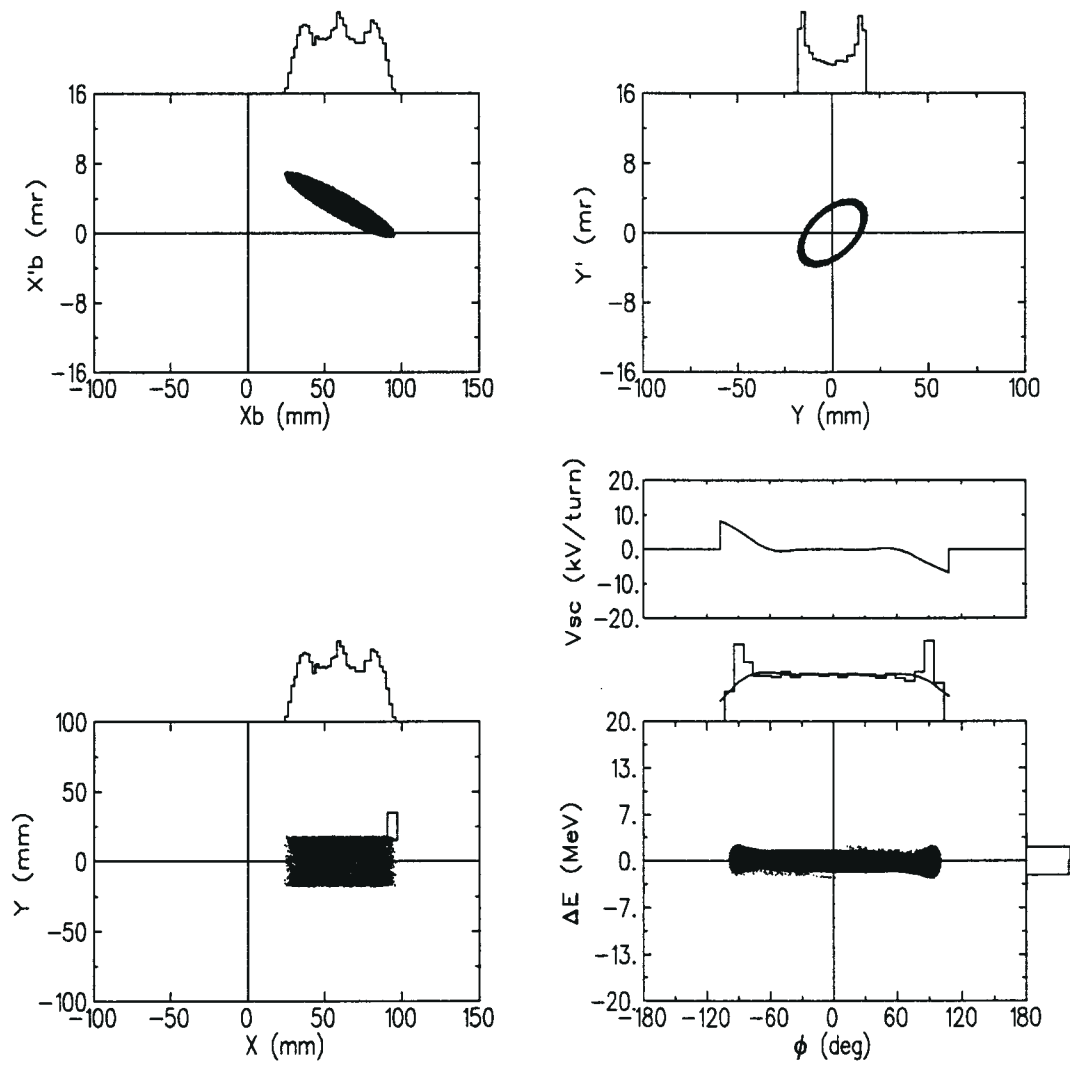


Figure 15: Snapshots at 1,200 turns. Barrier RF. No vertical painting.

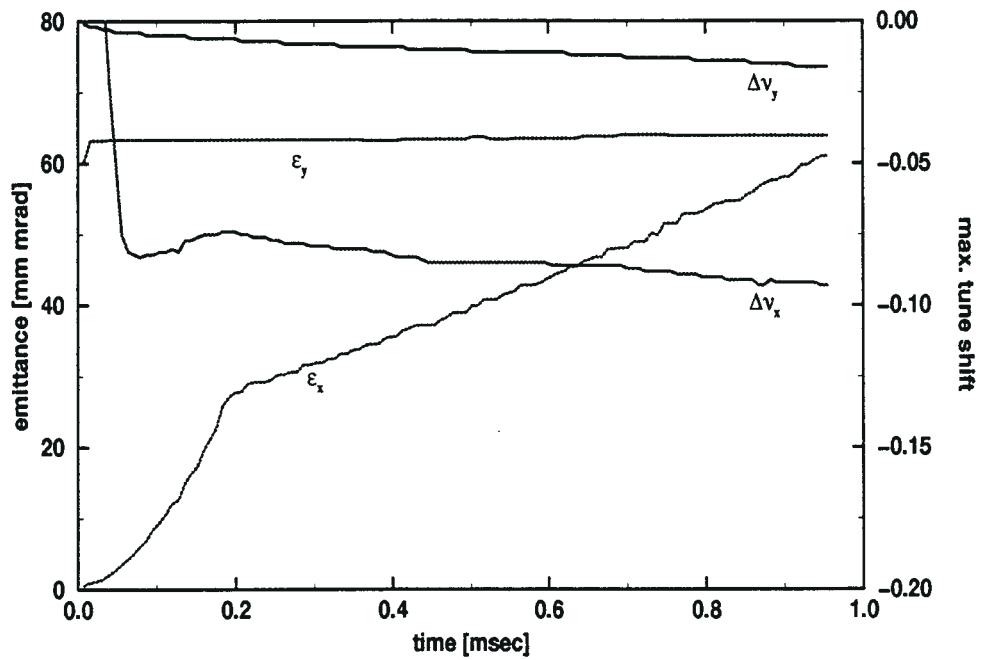


Figure 16: Transverse emittance and tune shift. Barrier RF. No vertical painting

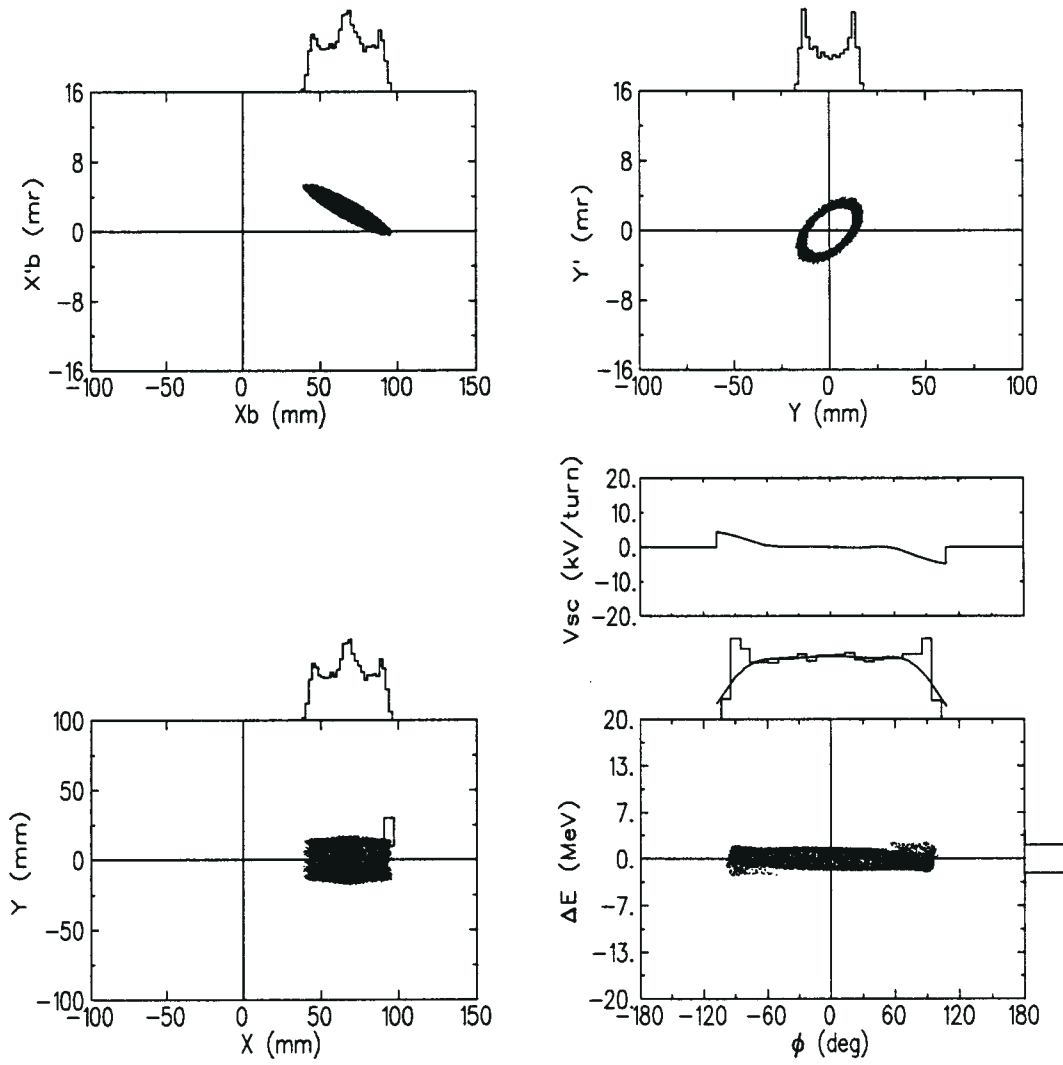


Figure 17: Snapshots at 600 turns. Barrier RF. Vertical painting

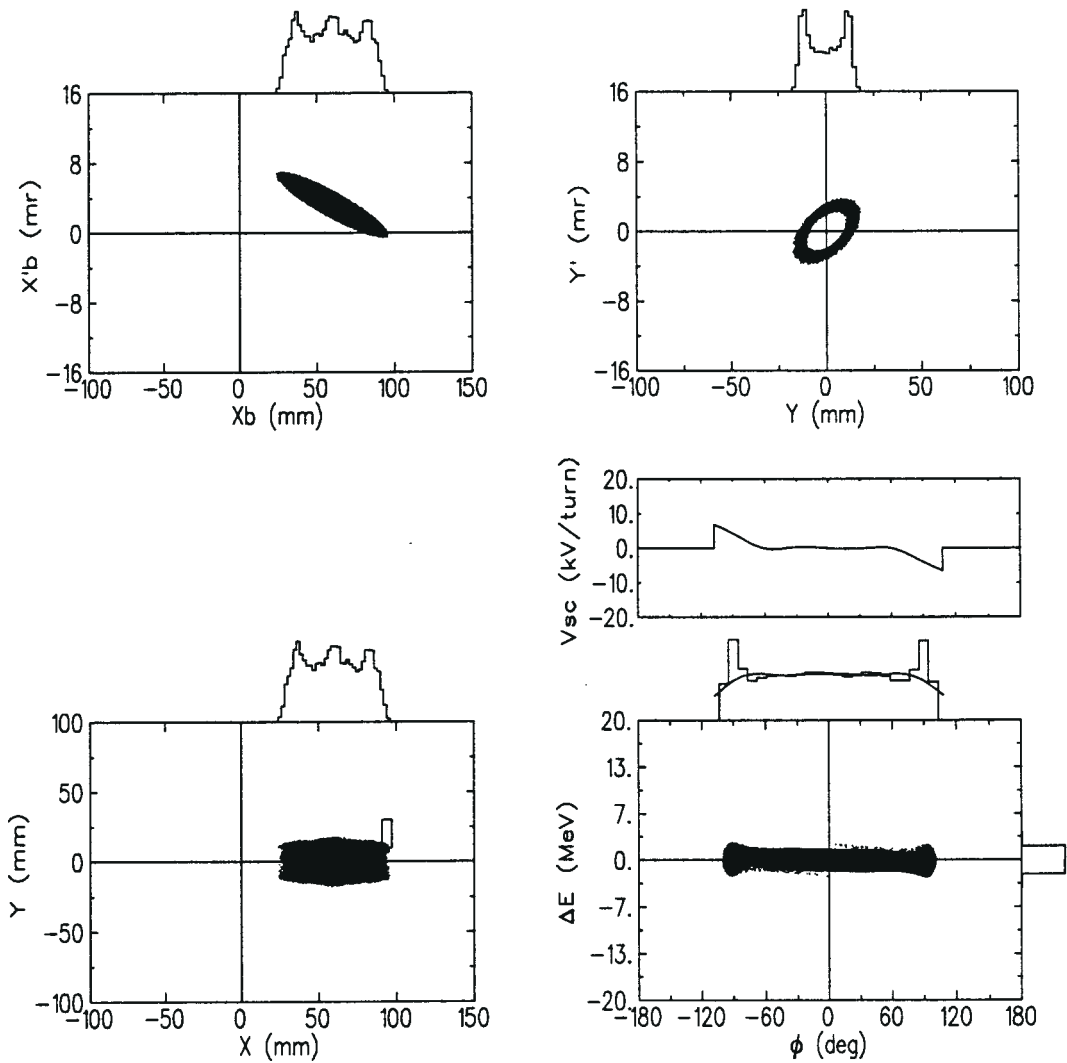


Figure 18: Snapshots at 1,200 turns. Barrier RF. Vertical painting.

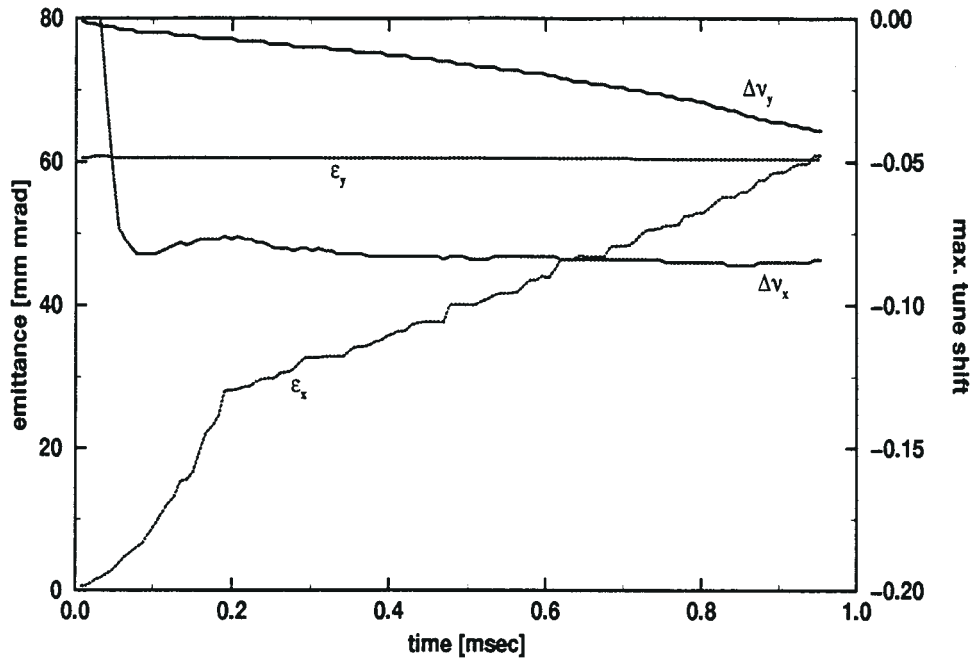


Figure 19: Transverse emittance and tune shift. Barrier RF. Vertical painting

The vertical acceptance remains centered on the vacuum chamber axis (no vertical bump) and the beam is steered inwards in the injection line.

Fig. 19 shows the radial and vertical emittance and tune shift. A comparison with Fig. 16 shows that in addition to the reduction of the radial tune shift due to the RF barrier, a negative increase of the vertical tune shift appears due to the thicker ring.

5.5. Common parameters of the simulation

Losses and foil traversals for the four cases above are given in Table. III A list of machine quantities are listed in Table. IV

Table III: Losses and foil hits.

No. of macroparticles = 12,000 Total charge = 1.042×10^{14}			
	lost at foil [%]	lost elsewhere	average foil hits
1.st harmonic RF:	1.962	$< 8 \times 10^{-5}$	3.612
1.st + 2.nd harmonic RF:	1.867	$< 8 \times 10^{-5}$	3.592
Barrier RF. No vertical painting:	1.783	$< 8 \times 10^{-5}$	3.557
Barrier RF. Vertical painting:	1.792	$< 8 \times 10^{-5}$	5.253

Table IV: Accumulator Ring Parameters.

Lattice Data		
Length of machine [m]	208.5480	
Average radius $L/2\pi$ [m]	33.19144	
Compaction factor	$8.5398473 \cdot 10^{-2}$	
γ_t	3.421960	
ν_x, ν_y	3.820629	3.779805
ξ_x, ξ_y	-3.549235	-3.598855
$\langle \beta_x \rangle, \langle \beta_y \rangle$ [m]	11.38699	10.61538
Synchronous particle		
γ, β	2.065803	0.8750274
Rev. frequency [MHz]	1.257872	
Rev. period [μ s]	0.7949935	
Radio Frequency		
f_{RF} [MHz]	1.257872	
Freq. slip factor η_0	-0.1489286	
Small ampl. synchrotron oscillations		
Frequency [KHz]	0.8706998	
Period [μ s], turns	1148.501	1444.668
Synch. tune	$6.9220067E-04$	
Coulomb scattering		
θ_{min} [mrad]	$2.9595762 \cdot 10^{-3}$	
Jackson θ_{max} [mrad]	36.05099	
Total cross section [mbarn]	$5.0355440 \cdot 10^8$	
Atom density	$1.1357147 \cdot 10^{23} \text{ cm}^{-3}$	
Scattering length [g/cm^2]	$3.9605231 \cdot 10^{-5}$	
Energy loss in foil [MeV]		
Max. per transfer	3.326661	
Average per traversal	$7.9077709 \cdot 10^{-4}$	
Nuclear scattering rate in foil		
	$4.2094880 \cdot 10^{-6}$	

6. Conclusions. Future work

A 6-dimension simulation with the code *Accsim* of the 1 GeV - 1 mA accumulator ring of the NSNS showed that a proton beam can be injected and captured for 1,200 turns, or 1 msec, with small controlled losses in the injection area, but with no subsequent losses to 10^{-4} .

The transverse space charge tune shifts never exceeded the design limit of -0.2.

Of the three RF scenarios investigated, Fundamental harmonic, Fundamental plus 2.nd harmonic and Barrier RF, the latter seemed able to further reduce the bucket area and the tune shifts.

These are already good workable solutions, however, work is in progress to further improve the design. The areas that need to be improved are:

- 1- Introduce in *Accsim* a complete impedance budget.
- 2- Add to the lattice sextupoles and/or octupoles.
- 3- Run with more macroparticles, say $10^5 - 10^6$.
- 4- Use a more realistic chamber wall profile.
- 5- Calculate the transverse tune spread. Compare *Accsim* results with a more refined mathematical model.
- 6- Improve the barrier cavity voltage waveform. Optimize bunch length.
- 7- Investigate momentum sweep during the injection.

7. References.

1. *Design of the NSNS Accumulator Ring and Beam Transport Systems (Pre-CDR Report)*. BNL NSNS Collaborative Design Team, October 25, 1996.
2. F.W.Jones. *User's Guide to Accsim*. TRIUMF Design Note TRI-DN-90-17, June 1990 (and later additions).
3. F.Ch.Iselin and J.Niederer. *The Mad Program. User's Reference Manual*. CERN/LEP-TH/88, July 13, 1988 (and later additions).
4. R.V.Servranckx, K.L.Brown, L.Schachinger and D.Douglas. *Users Guide to the Program Dimad*. SLAC Report 285 UC-28(A) May 1985.
5. A.G.Ruggiero, L.Blumberg, Y.Y.Lee, A.Luccio. *The NSNS Accumulator Ring*. BNL/NSNS Technical Note No.001, Upton, August 5, 1996.
6. L.N.Blumberg and Y.Y.Lee. *H⁻ Charge Exchange Injection into the 1 GeV NSNS Accumulator*. BNL/NSNS Technical Note No.003, Upton, November 1, 1996.
7. M.Blaskiewicz, J.M.Brennan and Y.Y.Lee. *RF Options for the NSNS*. BNL/NSNS Technical Note, Upton, November 15, 1996.
8. H.Schönauer. *Addition of Transverse Space Charge to Accsim Code*. TRIUMF Design Note TRI-DN-89-K50, August 1989.
9. H.Bruck. *Accélérateurs Circulaires de particules*. Presses Universitaires de France, Paris 1966.
10. E.Keil, E.Zeitler and W.Zinn. *Zur Einfach- und Mehrfachstreuung geladener Teilchen* Z.Naturforschg. 15a,1031,1960.

11. A.Hoffman. *Theoretical aspects of the behaviour of beams in accelerators and storage rings*. CERN 77-13,1977.
12. L.N.Blumberg, A.U.Luccio, A. VanSteenbergen, F.W. Jones. *A Pulsed Spallation Neutron Source. Solution with a 1.25 GeV Accumulator*. BNL-62391, UC-414, AGS/AD/96-2, Upton, October 30, 1995.